TOXICOLOGICAL SCIENCES **107(1)**, 206–219 (2009)
doi:10.1093/toxsci/kfn221
Advance Access publication October 29, 2008

Cadmium-Induced Differential Toxicogenomic Response in Resistant and Sensitive Mouse Strains Undergoing Neurulation

Joshua F. Robinson,* Xiaozhong Yu,* Sungwoo Hong,* William C. Griffith,* Richard Beyer,* Euvin Kim,* and Elaine M. Faustman*,†,‡,§,[1]

*Department of Environmental and Occupational Health Sciences, University of Washington, Seattle, Washington 98195; †Center for Ecogenetics and Environmental Health and Institute for Risk Analysis and Risk Communication, Seattle, Washington 98195; ‡Center on Human Development and Disability, Seattle, Washington 98195; and §Center for Child Environmental Health Risks Research, Seattle, Washington 98195

Received June 23, 2008; accepted October 8, 2008

Common inbred mouse strains, such as the C57BL/6 (C57) and the SWV, display differences in sensitivity to environmental teratogens during gestation. For example, the C57 is more sensitive than the SWV to cadmium (Cd) exposure during neurulation, inducing a higher incidence of neural tube defects (NTDs). Here, we report, using Cd as a model teratogen, the first large scale toxicogenomic study to compare teratogen-induced gene expression alterations in C57 and SWV embryos undergoing neurulation, identifying toxicogenomic responses that associate with developmental toxicity and differential sensitivity. Using a systems-based toxicogenomic approach, comparing Cd-exposed and control C57 and SWV embryos (12- and 24-h postinjection [p.i.] [gestational day 8.0, ip]), we examined differentially expressed genes at multiple levels (biological process, pathway, gene) using Gene Ontology (GO) analysis, pathway mapping and cross-scatter plots. In both C57 and SWV embryos, we observed several gene expression alterations linked with cell cycle–related classifications, however, only in the C57 we observed upregulation of p53-dependent mediators Ccng1 and Pmaip1, previously associated with cell cycle arrest, apoptosis and NTD formation. In addition, we also identified a greater reduction in expression of nervous system development-related genes (e.g., Zic1, En2, Neurog1, Elavl4, Metrn, Nr2f1, Nr2f2) in the C57 compared to the SWV (12-h p.i.). In summary, our results indicate that differences in Cd-induced gene expression profiles between NTD resistant and sensitive strains within enriched biological processes (including developmental and cell cycle–related categories) associate with increased sensitivity to developmental toxicity as determined by observations of increased NTD formation, mortality (resorptions) and reduced fetal growth. Such observations may provide more detailed and useful mechanistic clues for identification of differences in life-stage specific teratogenic response.

Key Words: **cadmium; exencephaly; mouse; neural tube defects; toxicogenomics; SWV.**

Neurulation represents the beginning of neurogenesis, occurring approximately during gestational days (GD) 8–10 in the mouse and GD 21–26 in humans. Perturbations in this complex conserved process result in neural tube defects (NTDs), representing the second most common birth defect in the human population (Nassau and Drotar, 1997). A majority of NTDs appear to be the result of both genetic predisposition and environmental exposure (Frey and Hauser, 2003). Studies comparing differences in sensitivity to environmental teratogens between inbred mouse strains suggest a multifaceted challenge to identify factors that confer sensitivity. Teratogen-dependent differences in sensitivity have been observed between the C57BL/6 (C57) and the SWV mouse strains when exposed during early development (GD 7–10). Specifically, the SWV strain is more sensitive to NTDs caused by phenobarbital, valproic acid, and hyperthermia as compared to the C57 strain (Finnell *et al*., 1986, 1987; Naruse *et al*., 1988), whereas the C57 is more sensitive than the SWV to cadmium (Cd) and arsenic exposures (Hovland *et al*., 1999; Machado *et al*., 1999). Follow-up genome linkage studies comparing C57 and SWV strains exposed to specific teratogens during development suggest that both maternal and fetal components underlie observed differences in sensitivity between these two strains (Hovland *et al*., 2000; Lundberg *et al*., 2003, 2004).

Cd is ubiquitous in the environment due to both natural and anthropogenic sources. Although chronic exposure to Cd is associated with cancer and bone, lung, and renal damage, classification of Cd as a human teratogen remains controversial. Developmental effects, such as reduced birth weight, have been associated with Cd exposure *in utero* in humans (Ronco *et al*., 2005), however, recent epidemiological studies have not demonstrated the potential ability of Cd to induce birth defects such as NTDs (Brender *et al*., 2006). Nevertheless, in rodent models, Cd is a developmental teratogen able to induce lethality and a wide range of teratogenic effects (Ferm, 197l), dependent on strain, dose, and time of administration (Hovland *et al*., 1999). In studies using doses ($\geq$ 2 mg/kg body weight (BW)) and injection methods (ip, sc), maternal exposure(s) to Cd

Presented in part at the annual meeting of the Society of Toxicology, March 25 to March 29, 2008, Charlotte, NC.

[1] To whom correspondence should be addressed at Department of Environmental and Occupational Health Sciences, 4225 Roosevelt Way NE Suite 100, University of Washington, Seattle, WA 98105. Fax: (206) 685-4696. E-mail: faustman@u.washington.edu.

during the period of neurulation results in disruption of neural tube closure in the cranial region, causing the NTD, exencephaly (Ferm and Carpenter, 1968).

Although the mechanistic etiology of how Cd induces exencephaly is poorly understood, it likely comprises a complex series of molecular events dependent on several factors. In animal models, Cd accumulates in maternal extraembryonic tissues (visceral yolk sac and choriallantoic placenta) (Dencker, 1975) resulting in changes in nutrient transport and zinc distribution critical for the neurulation period (Danielsson and Dencker, 1984). Cd may also directly impact the embryo, localizing in cells of the neural tube, limb buds and gut in a time and dose dependent manner (Christley and Webster, 1983). Similar to other known teratogens (valproic acid, hyperthermia, arsenic), exposure to Cd during neurulation has been linked to a wide range of cellular and biochemical alterations, including markers of oxidative stress (lipid peroxidation and DNA damage) (Fernandez *et al*., 2004; Paniagua-Castro *et al*., 2007), cell cycle perturbations marked by upregulation of cell cycle regulators (p53, Cdkn1a) (Fernandez *et al*., 2003), apoptosis (Fernandez *et al*., 2003), and altered expression of key developmental signaling molecules (Fernandez *et al*., 2004).

The emergence of microarray technologies and other genomic approaches has rapidly advanced the field of toxicology, providing a more efficient means to explore the mechanistic effects of chemicals and to investigate the etiology of genetically susceptible populations. In this study, using Cd as a model teratogen, we report the first microarray study to assess teratogen-induced alterations in gene expression coinciding with cranial neural tube closure comparing sensitive and resistant mouse embryos to identify toxicogenomic responses that underlie NTD development and potential mechanisms of differential sensitivity between these two strains. Assessing gene expression changes 12- and 24-h maternal postinjection (p.i.) (GD 8.0, ip), we report Cd to induce common and unique gene expression alterations representing several biological processes (GO classifications). We demonstrate that differences in Cd-induced gene expression profiles within development and cell cycle–related categories associate with developmental toxicity and discuss the potential for specific genes involved in nervous system development (i.e., Zic1, En2, Nr2f2, Elavl4) and cell cycle regulation (i.e., p53, Cdkn1a, Ccng1, Pmaip1) to associate with observed differences in Cd sensitivity.

METHODS

Animals and cadmium exposure. Colonies of C57BL/6J (C57) and SWV strains were maintained at the University of Washington, Department of Environmental and Occupational Health Sciences. C57 mice were supplied from Jackson laboratories and SWV colonies were established from mice acquired from Dr Phillip Mirkes (University of Washington, Department of Pediatrics), originally provided by Dr. Richard Finnell (Texas A&M University). Animal care and all experiments were conducted in agreement with the University of Washington Institutional Animal Care Committee. Housed in filter covered transparent plastic cages, animals were maintained in climate-controlled rooms under an alternating 12-h light/dark cycle. Water and food were available *ad libitium*. Timed matings were produced by placing individual male mice into cages containing two females. Copulatory plugs were identified in the early morning (8:00 A.M. ± 0.5 h) the following day and designated as GD 0. Pregnant mice were administered single doses via ip injection on GD 8.0, 8:00am (± 1 h), with either Cd chloride (4 mg/kg/BW, Alfa Aesar, Ward Hill, MA) dissolved in deionized water (working concentration of 2mM), or water (control) (10 μl/g). The administrative time and dose were selected based on previous observations indicating exposure to Cd on GD8 results in increased incidence of NTDs (exencephaly) in C57 and SWV fetuses and furthermore, the C57 displays higher sensitivity to Cd-induced NTDs (> 2×) compared to the SWV (Hovland *et al*., 1999).

Developmental assessment (GD 18). Pregnant C57 and SWV mice were euthanized on GD18 via inhalation of isofluorane and cervical dislocation. The uterus was removed from each dam. Fetuses were sacrificed by overexposure to isofluorane. The number of total fetuses, implantation sites, and resorptions were recorded. Individual fetuses were removed and recorded for observations of gross malformations, body weight, head diameter (length from front to back) and crown rump length.

RNA isolation. Separate pregnant C57 and SWV females were euthanized on GD 8.5 and GD 9.0, 12 and 24-h p.i., respectively. The uterine horns were extracted from the abdomen region and placed in cold CMF-EBSS (Gibco, Carlsbad, CA). Embryos were isolated, washed in cold CMF-EBSS, placed in liquid nitrogen, and stored at −80°C. Prior to storage, embryos were quickly assessed for closure of the neural tube in the mid/hind brain region. Complete pooled litters were kept separate. Embryos were placed in 500 μl of RTL Cell Lysis buffer (Qiagen, Valencia, CA) and lysed with a 30G needle to homogenize the tissue. RNA was purified using the RNAeasy kit (Qiagen). Quality was assessed using the "6000" assay on the 2100 Bioanalyzer (Agilent Technologies, Palo Alto, CA). Time points were chosen to reflect closure of the cranial neural tube (Table 2) and correspond with previous morphological and molecular observations of Cd toxicity (Fernandez *et al*., 2003, 2004; Webster and Messerle, 1980).

Oligonucleotide microarrays. We assessed for Cd-induced alterations in gene expression 12- and 24-h p.i. using the Mouse Codelink Uniset I platform. Oligonucleotide microarray analysis was completed at the Fred Hutchinson Cancer Research Center Functional Genomic Laboratory following the manufacturer suggested protocol for the Codelink Mouse Uniset I 20K oligonuceotide array (GE Healthcare Life Sciences, Uppsala, Sweden). For each treatment (Cd or vehicle), three (GD 8.5, 12 h) or four (GD 9.0, 24 h) independent litters were collected (28 total). One separate pooled litter was used for each sample. First and second strand cDNA synthesis was completed using 1 μg of total RNA. Mixed with bacterial control mRNAs and T7-(dT)24 primers, samples were denatured at 70°C for 10 min. Dithiotreitol, deoxynucleotide triphosphates (dNTPs), and Superscript II RnaseH-reverse transcriptase (Gibco, Carlsbad, CA) were added and samples were incubated at 42°C. Additional dNTPs, RnaseH, and DNA polymerase were added to the mix and incubated for 2 h at 16°C. Double-stranded cDNA was purified using a QIAquick spin column (Qiagen, Valencia, CA). cRNA synthesis was completed by *in vitro* transcription which consisted of mixing purified ds cDNA, ATP, guanosine triphosphate (GTP), cytidine triphosphate, uridine triphosphate (UTP), biotin-11-UTP, and the enzyme mixture and incubating at 37°C for 14 h (Amersham Biosciences, Piscataway, NJ). cRNA was purified using the RNAeasy kit (Qiagen, Valencia, CA). RNA quality was assessed using the Agilent 2100 Bioanalyzer (Agilent Technologies). Less than 10% of the amplified product, 10 μg was used for hybridization. cRNA was fragmented at 94°C for 20 min and then, loaded into its respective slide chamber. Hybridization was performed for 18 h at 300 rpm (shaker-incubator speed) and 37°C. Arrays were washed with 0.75× (0.10M Tris-HCl, pH 7.6; 0.15M NaCl;

0.05% Tween 20) (TNT) for 1 h at 46°C and then, incubated with AlexaFlour 647-streptavidin (Molecular Probes, Eugene, OR) for 30 min. Following four washes in 1× TNT and two washes in 0.05% Tween-20, slides were dried at 2000 rpm for 3 min and checked for smears. Finally, arrays were scanned on the Axon GenePix 4000 Scanner (Axon Instruments, Union City, CA) at 635 nm, PMT 600 V and 10μM resolution.

Data processing. Expression values were generated using Codelink Expression Analysis software v2.0 (GE Healthcare Life Sciences, Uppsala, Sweden) for all 20,290 probes. Spot quality, control probe characteristics, and median array intensities were examined to identify potential reading misalignment, improper hybridization or other abnormalities. Raw intensities were normalized using the global median (as recommended by Codelink) and transformed by log base 2 (Bioconductor [limma], www.bioconductor.org). False discovery rates were computed to control for multiple testing.

Identification of significantly altered genes and enriched gene ontology classifications. As observed in Figure 1, we used a systems-based approach to identify significant Cd-induced gene expression alterations and their respective Gene Ontology (GO)–based classifications in the C57 and the SWV. We employed three linear models to detect genes that were (1) differentially expressed based on the effect of time and Cd treatment in the C57 (Model 1), (2) differentially expressed based on the effect of time and Cd treatment in the SWV (Model 2), and (3) either commonly or differentially expressed based on the effect of time, Cd treatment, and strain (Model 3).

- **Model 1:** $\log2[\text{Exp}_n]\text{C57BL/6J} = B_0 + B_{\text{Time}}x_1 + B_{\text{Cd}}x_2 + B_{\text{Time\_Cd}}x_1x_2$
- **Model 2:** $\log2[\text{Exp}_n]\text{SWV} = B_0 + B_{\text{Time}}x_1 + B_{\text{Cd}}x_2 + B_{\text{Time\_Cd}}x_1x_2$
- **Model 3:** $\log2[\text{Exp}_n]\text{C57BL/6J\_ SWV} = B_0 + B_{\text{Time}}x_1 + B_{\text{Cd}}x_2 + B_{\text{Strain}}x_3 + B_{\text{Time\_Cd}}x_1x_2 + B_{\text{Time\_Strain}}x_1x_3 + B_{\text{Cd\_Strain}}x_2x_3 + B_{\text{Time\_Cd\_Strain}}x_1x_2x_3$

Cross-scatter plots displaying the magnitude and directionality of effect associated with Cd exposure in C57 and SWV strains 12- and 24-h p.i were constructed using all genes identified to be significantly altered with Cd (Models 1–3, $p < 0.01$). Based on the Cartesian coordinate system, quadrant I (top right, upregulated) and quadrant III (lower left, downregulated) present gene alterations with common directionality in C57 and SWV strains. In quadrant II (up in SWV, down in C57) and quadrant IV (up in C57, down in SWV), we present gene expression alterations with differing directionality of Cd response comparing C57 and SWV strains at each respective time point (12- or 24-h p.i.). Symbols indicate strain specificity of significant Cd-induced gene expression alterations based on our three linear models (Model 3 (□), 2 (○) or 1(Δ), $p < 0.01$). Genes identified to be significantly impacted by Cd in Model 3 may not necessarily demonstrate significant Cd effects in Model 1 and/or Model 2 ($p < 0.01$), thus, we labeled genes first by Model 3 and then, Model 1 or Model 2, respectively.

GO analysis (Doniger *et al.*, 2003) was conducted to explore over-representation of GO gene categories (biological process, molecular function, and cellular component) within significantly differentially expressed genes identified to be altered with Cd exposure for each of our three models (ANOVA, B_{Cd}, $p < 0.01$, Models 1–3). In addition, GO analysis was completed for genes identified to be differentially impacted by Cd between the two strains (ANOVA, $B_{\text{Cd\_Strain}}$ $p < 0.01$, Model 3). Significant GO categories were determined based on a permutation value cutoff ($p < 0.02$), a *Z*-score ($Z > 2$) and a minimum of three genes altered within each specific GO ID. Pathway analysis was conducted via Ingenuity Pathway Analysis (Ingenuity Systems, Redwood City, CA) (results not shown). Genes within nervous system development (GO:7399) and cell cycle (GO:7049, 45786) related GO categories were examined using cross-scatter plots of all genes identified to be significantly altered with Cd exposure (B_{Cd}, $p < 0.01$, Models 1–3). Genes were presented as symbols (Model 3 (□), 2 (○) or 1(Δ), $p < 0.01$) representing strain specificity of significant Cd effect(s). Using the GO-based application, GO-Quant, which quantitatively describes dose- and time-dependent alterations across multiple genes within selected GO categories, we quantified the impact of Cd on nervous system development gene expression in C57 and SWV embryos by calculating the average magnitude in change (fold ratio) associated with Cd in all up or downregulated genes (Models 1–3, $p < 0.01$, 54 genes total) at each time point (GO-Quant, Yu *et al.*, 2006). We examined potential common and differential interactions between p53 and genes involved in cell cycle/apoptotic regulation using the canonical Ingenuity p53 Signaling pathway (Ingenuity Systems), color coded based on strain specificity of Cd response (B_{Cd}, $p < 0.01$, Models 1–3).

Secondary confirmation of RNA expression using real-time quantitative reverse transcription polymerase chain reaction. To verify Cd-induced gene expression alterations identified by the Codelink microarray platform, we conducted real-time quantitative reverse transcription polymerase chain reaction (qRT-PCR) (Taqman, Applied Biosystems, Inc., Foster City, CA) for four genes of interest and one housekeeping gene: Cdkn1a, Pmaip1, En2, Neurog2, and Gapdh. Total RNA from litters of C57 and SWV embryos was collected and purified under the same experimental conditions as in our microarray study (12-h p.i. only). cDNA synthesis was completed using 1ug of total RNA using Oligo(dT)12–18 and Superscript II Reverse Transcriptase (Gibco, Carlsbad, CA). PCR reactions were performed using 2 μl of cDNA, forward and reverse primers (250nM), TaqMan probe (167nM) and TaqMan Fast Universal Master Mix (Pmaip1) or TaqMan Gene Expression Master Mix (Applied Biosystems, Inc., Foster City, CA). Amplification and detection was conducted using the ABI PRISM 7700 system (Applied Biosystems, Inc., Foster City, CA) with the following PCR reaction profile: 1 cycle of 95°C for 15 s, 40 cycles of 95°C for 1 s, and 60°C for 20 min. Values reported represent fold change comparisons between raw intensity values adjusted by Gadph of Cd-exposed and control C57 or SWV embryos. Two-sided *t*-tests were completed between control and Cd-exposed embryos to identify significant effects. All probes are listed in Supplementary Table 2.

RESULTS

Effects of Cd on Growth and Development (GD 18)

Table 1 summarizes developmental characteristics of C57 and SWV fetuses exposed to Cd versus control assessed on

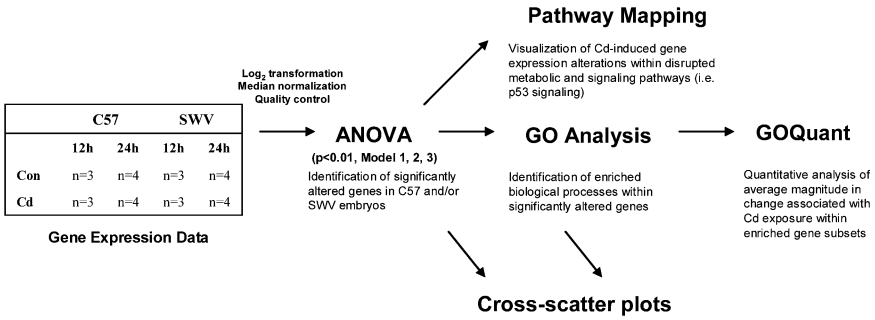

FIG. 1. Toxicogenomic approach to identify differential Cd-induced alterations in gene expression in C57 and SWV embryos.

GD18. In the C57, Cd exposure led to a higher rate of resorptions compared to control ($p < 0.05$). In addition, Cd-treated C57 embryos showed a reduction in overall development, including significant decreases in body weight and head diameter ($p < 0.05$). In the SWV, we did not observe any significant impact on embryonic development based on the endpoints assessed.

Cd-Induced Exencephaly

The mean percentage of fetuses with exencephaly on GD18 in C57 litters (33.1%) is greater compared to SWV litters (4.6%, $p < 0.005$) (Table 1), reflecting a significant ($p < 0.005$) difference between strains.

The Effect of Cd on Cranial Neural Tube Closure

As shown in Table 2, Cd exposure altered neural tube closure (mid-hind/brain region) in both C57 and SWV embryos. At 12-h p.i., we observed a significant increase ($p < 0.05$) in the percentage of neural tubes open in the C57 with Cd (93.8 ± 4.1%) compared to control (63.5 ± 13.1%), whereas in the SWV, no significant changes were observed. At 24-h p.i., we observed a 74% or 19× increase in open neural tubes in the C57 with Cd compared to control ($p < 0.0005$) and a 48% or 6× increase in the SWV with Cd compared to control ($p < 0.05$).

Cd-Induced Gene Expression Alterations and in C57 and SWV Embryos Undergoing Neurulation

In Figure 2 we show the distribution of significant Cd-induced gene expression alterations in C57 and SWV embryos over time (12-, 24-h p.i.). Venn diagrams (Fig. 2A) indicate gene expression alterations identified due to each effect assessed (i.e., time, treatment, strain, interaction variables) within linear ANOVA Models (1–3).

In Models 1 and 2, we observed a total of 374 (148↑, 226↓) and 739 (500↑, 139↓) genes to be significantly altered by Cd exposure (B_{Cd}, $p < 0.01$) in C57 and SWV embryos across time (12, 24 h), respectively. Within the 374 genes identified to be significantly altered by Cd exposure in the C57, our Venn diagram shows 20 (14 + 6) genes to also show a significant time effect (B_{Time}, $p < 0.01$) and 84 (14 + 70) genes to show a significant Time_Cd interaction effect (B_{Time_Cd}, $p < 0.01$). Similarly in the 739 genes identified to be altered by Cd in the SWV, we observed 450 and 453 to display significant Time and/or Time_Cd interaction effects ($p < 0.01$).

In our three-way ANOVA model assessing the effect of time, treatment, strain and their respective interactions (Fig. 2A, Model 3), we identified 658 genes to be commonly altered due to Cd treatment (B_{Cd}), 123 genes to have a significant interaction between treatment and strain (i.e., genes that were impacted by Cd differentially between C57 and SWV embryos) (B_{Cd_Strain}, $p < 0.01$) and 75 genes with an interaction between all three primary variables ($B_{Cd\_Time\_Strain}$) (i.e., genes differentially expressed between treatment, time and strain).

In Figures 2B and 2C, we show cross-scatter plots of all genes identified to be significantly impacted by Cd (B_{Cd}, $p < 0.01$, in either Model 1, 2, or 3) presenting the fold change difference in gene expression comparing Cd-exposed and control C57 and SWV embryos using a log 2 scale ($1 = 2^1 \times$ fold change) scale. Labeled genes represent a selection of genes with large Cd effect(s) in terms of magnitude of response (~2× fold change or greater in one of the two strains). In total, we identified 1212 genes to be altered due to Cd exposure in C57 and/or SWV embryos (B_{Cd}, $p < 0.01$, in either Models 1, 2, or 3). Cross-scatter plots suggest several significant common (□) up- and downregulated gene expression alterations as well as unique Cd-induced alterations in either the C57 (Δ) or SWV (○) based on the significance of Cd effect (p value, symbol), magnitude (fold change) and directionality of response. Following 12-h exposure (Fig. 2B [quadrant I]), we observed upregulation of Cebpz in both C57 (↑2.1×) and SWV (↑2.4×) strains. Additionally, in Figure 2B we identified genes that were significantly altered in only one of the two strains, such as Mglap and Fabp7 which were significantly altered in only the C57 (Δ) (↑7.3×) (quadrant IV) and (↓7.4×) (quadrant III), respectively. Although in Figure 2B, Pcdha4 (↑6.6×) (quadrant I) was significantly altered in only the SWV (○). At 24-h p.i. (Fig. 2C), we observed upregulation of Cdkn1a (↑1.9×) in the C57 (Δ) (quadrant I)

TABLE 1
Developmental Impact of Cadmium in C57 and SWV Fetuses Assessed on GD18

Strain	Exposure	# *F*	Imp/litter	RR/litter	BW (g)	HD (mm)	CR (mm)	NTD (exencephaly)
C57	Control ($n = 12$)	90	8.2 ± 0.3	8 ± 3%	1.08 ± 0.02	10.3 ± 0.1	20.8 ± 0.3	0%
	Cadmium ($n = 8$)	59	9.9 ± 0.6	32 ± 4%*	0.99 ± 0.03*	9.7 ± 0.2*	20.6 ± 0.3	33.1 ± 9.2%#
SWV	Control ($n = 8$)	98	12.8 ± 0.7	4 ± 3%	0.93 ± 0.03	10.5 ± 0.1	20.3 ± 0.6	0%
	Cadmium ($n = 7$)	87	13.1 ± 0.3	5 ± 2%	0.97 ± 0.05	10.3 ± 0.1	20.5 ± 0.5	4.6 ± 3.0%

Note. Following exposure (GD 8.0), on GD 18, individual fetuses (# *F*) were isolated and examined for gross malformations (i.e., exencephaly), body weight (BW), and growth characteristics (head diameter [HD] and crown rump length [CR]). In addition, implantation sites (Imp), and resorption rates (RR) for each litter were recorded. All measurements are based on litter averages. Data are shown as mean ± SEM. An asterisk (*) signifies significance between Cd-treated and control ($p \leq 0.05$, one-sided *t*-test). The hash (#) indicates differently affected by Cd exposure between strains ($p \leq 0.005$).

TABLE 2
The Impact of Cadmium Exposure on Cranial Neural Tube Closure in C57 and SWV Embryos

Strain	Exposure	GD 8.0 + 12 h	GD 8.0 + 24 h
C57	Control	63.5 ± 13.1%	4.2 ± 2.7%
	Cadmium	93.8 ± 4.1%*	77.9 ± 10.0%***
SWV	Control	71.1 ± 16.7%	10.3 ± 7.7%
	Cadmium	66.3 ± 16.7%	58.2 ± 11.3%*

Note. The mean percentage of open neural tubes (mid/hind brain region) in each litter of Cd-exposed and control C57 and SWV embryos was assessed for closure on GD 8.5 and GD 9.0 corresponding with GD 8.0 + 12-h p.i. and GD 8.0 + 24-h p.i., respectively. All measurements are based on litter averages ($n = 6$–10 for each group). Data are shown as mean ± SEM. Significant effects were identified between control and Cd-exposed values at each time point using a two-sided *t*-test (*$p < 0.05$, ***$p < 0.0005$).

and upregulation of Olfr45 (↑3.1×) (quadrant II). In general, in terms of magnitude of response, we observed more increased alterations in gene expression due to Cd at 12-h p.i. compared to 24-h p.i. (B_{Cd}, $p < 0.01$, Models 1–3).

In Figures 3A and 3B, we present cross-scatter plots of all 123 genes identified to be significantly differentially impacted by Cd between C57 and SWV embryos (B_{Cd_Strain} $p < 0.01$, Model 3). At 12-h p.i., we observed several genes to be upregulated in SWV and downregulated in the C57 (quadrant II). Examples include Lhx9, Ecel1, H28, Zwim5, and Shd. Likewise, we observed genes to be downregulated in the SWV and upregulated in the C57 (e.g., Mglap, Hmgcs2, 3830408610Rik, Ccl19, Npn3) (Fig. 3A, quadrant IV). At 24 h (Fig. 3B), the magnitude of Cd response did not differ between C57 and SWV to the degree observed at 12 h within this subset of genes.

GO Analysis of Cd-Induced Gene Expression Alterations

As shown in Table 3, enriched biological processes were identified within genes impacted by Cd in C57 or SWV embryos (Models 1 and 2, B_{Cd}, $p < 0.01$). For example, in the C57, we identified the biological process "nervous system development" (Path: 0.0.12.13.16.8/GOID: 7399) to be over-represented, with 21 nervous system development genes/374 genes identified to be significantly altered by Cd exposure in the C57 (Model 1, B_{Cd}, $p < 0.01$). In the SWV, we also observed 30 nervous system development genes/739 genes to be significantly altered; however, this category was not identified to be enriched based on our set criteria of p value ($p < 0.02$) and Z-score ($Z > 2.0$). Based on the GO hierarchy, we identified nervous system development (*) and cellular development-related processes to be enriched in only the C57. In the SWV, we observed overrepresentation of regulation of cellular process, protein kinase cascade, metabolism and DNA damage-related classifications (Table 3). In both strains, we identified enrichment of GO IDs within the broad scope of cellular proliferation, however these GO IDs differed between strains due to the specificity of genes altered in each strain. In the C57, we observed overrepresentation of cell cycle arrest-related categories (^), whereas in the SWV, we observed cell cycle and cell cycle process ($). Based on our set criteria, GO analysis did not indicate an overlap in response between C57 and SWV in any of the 87 unique GO categories (biological processes) identified to be altered in one of the two strains. In Supplementary Table 3, we identified enriched GO biological processes impacted by Cd, independent of strain (Model 3, B_{Cd}, $p < 0.01$). We observed overrepresentation of protein kinase cascade, cell cycle, macromolecule metabolism, response to ultraviolet (UV) and DNA damage-related categories as observed in Table 3 in the C57 or SWV. In addition, we identified new enriched processes related to microtubule polymerization and gastrulation. The majority of these categories overlapped with GO categories identified in the SWV (Model 2).

We conducted GO Analysis for the 123 genes identified to be differentially impacted by Cd between the two strains (B_{Cd_Strain} $p < 0.01$, Model 3). We identified one biological process to be significantly enriched within this subset (regulation of transcription\, DNA dependent) (not shown). The corresponding 18 genes are listed with fold change ratios in Supplemental Table 1.

We further investigated genes within nervous system development (GO:7399) and cell cycle (GO:7049, 45786) related GO categories via cross-scatter plots for all genes identified to be significantly altered with Cd exposure (B_{Cd}, $p < 0.01$, Models 1–3). These categories were of interest due to differential representation in Cd-altered genes comparing C57 and SWV embryos, GO analysis suggesting overrepresentation in the C57 (development, cell cycle arrest) or SWV (cell cycle) and prior findings associating these gene-linked processes with NTDs (Harris and Juriloff, 2007).

Impact of Cd on Nervous System Development Gene Expression

As shown in Figures 4A and 4B, we examined Cd-induced gene expression changes within genes involved in nervous system development using cross-scatter plots. Following 12-h p.i. (Fig. 4A, quadrant I), Cd-induced upregulation of Celsr3, Sema4d, Catnb, and Map3k7 in both strains represented by (□). In the C57 (Δ), Cd significantly downregulated expression of Pard3b, Elavl4, En2, Olig3, Crym, Slit3, Neurog1, Foxp2, Metrn, Nr2f1, Nr2f2, Zic1, and Zic2 (Fig. 4A, quadrant III). At 12-h p.i. (Fig. 4A, quadrant II), Ecel1 was significantly altered in both strains (□), however, significantly differed in response between C57 and SWV (Model 3, B_{Cd_Strain}, $p < 0.01$). In the C57, Ecel1 (12-h p.i.) was downregulated (↓2.5×), whereas in the SWV Ecel1 was upregulated (↑2.9×). Whereas at 24-h p.i. (Fig. 4B, quadrant III), we observed approximately equal reduction of Ecel1 in C57 (↓1.6×) and SWV (↓1.5×)

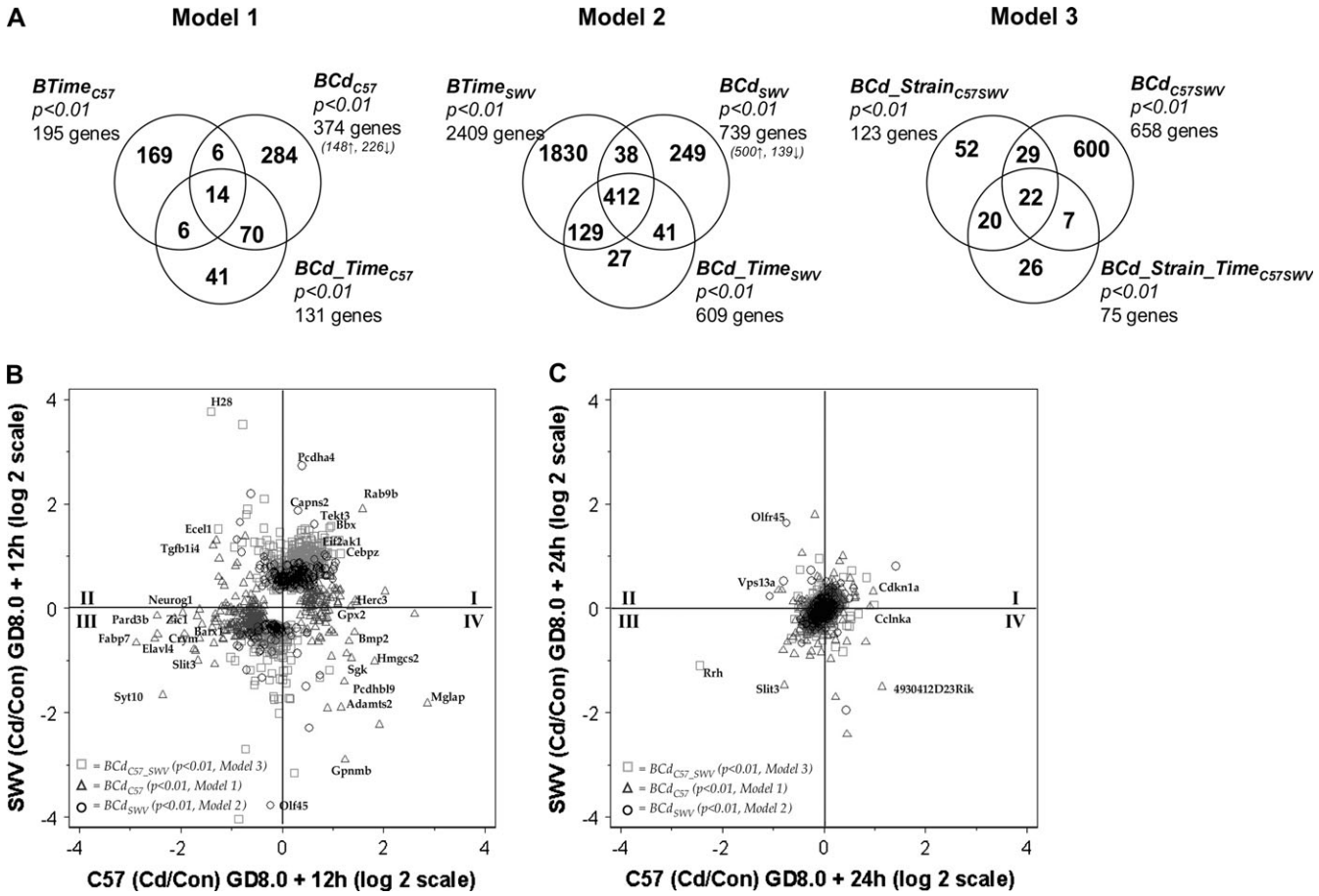

FIG. 2. ANOVA distributions of Cd-induced gene expression alterations in C57 and SWV embryos. Venn diagrams (A) display the distribution of genes identified to be significantly altered due to selected effects within each one of the three models. Scatter plots display the magnitude of change (Cd/Con) between Cd and control in differentially expressed genes in C57 and SWV embryos (12-h [B] and 24-h [C] p.i.). Genes were identified as statistically significant due to a significant BCd term ($p < 0.01$) in one of our three ANOVA models assessing for genes that are commonly or uniquely altered in the two strains. Genes identified by one of our three ANOVA models are displayed as (A) B_{Cd} ($p < 0.01$), in both strains (light gray squares), (B) B_{Cd} ($p < 0.01$), C57BL/6J only (dark gray triangles) and (C) B_{Cd} ($p < 0.01$), SWV only (black circles).

embryos. In addition, at 24-h p.i., we observed downregulation of Slit3, Crym, and Neurog1 (24-h p.i.) in the C57, with a similar response in the SWV (Fig. 4B, quadrant III).

As shown in Figure 4C, using GO-Quant, we calculated the average fold change (Cd/Con) associated with all nervous system development-related up (or down) regulated genes stratified by strain and time. In total, we observed 54 genes to be significantly altered by Cd in either of the two strains (Models 1–3, $p < 0.01$) which were linked with the GO nervous system development classification. At 12-h p.i., we observed 30/54 and 31/54 upregulated genes in the C57 and SWV, respectively. The SWV showed a greater average increase in expression within this subset of genes (~1.6×) compared to the C57 (1.3×). In contrast, in genes identified to be downregulated (12-h p.i.), we observed a larger degree of inhibition on average in the C57 (~↓2.0×) compared to the SWV (~↓1.3×). At 24-h p.i., differential Cd effects between strains were not observed (magnitude and the amount of up-/downregulated genes). In general, we observed an increase Cd response (magnitude of fold change) in nervous system development-related gene expression 12-h p.i. compared to 24-h p.i. for both up- and downregulated genes.

Impact of Cd on Cell Cycle Gene Expression

As illustrated in Figure 5, Cd-induced gene expression alterations in cell cycle–related genes in C57 and SWV embryos. At 12-h p.i. (Fig. 5A) we observed common (□) upregulation of p53, Ccne2, Wee1, Cables1, Eif2ak1, and Hdac7a (quadrant I). In only the C57 (Δ) (12-h p.i.), Cd-induced Ak1, Cdkn1a, Pmaip1, and Ccng1 gene expression (quadrant I, IV). Within the SWV (○), we observed alterations in H2afx and Sipa1 (quadrant II). At 24-h p.i., we observed sustained downregulation of Ccng1 and Cdkn1a in the C57 (Fig. 5B, quadrant I). Ccng1 and Ak1 were identified to be significantly differentially expressed between C57 and SWV embryos with Cd exposure (Model 3, B_{Cd_Strain}, $p < 0.01$).

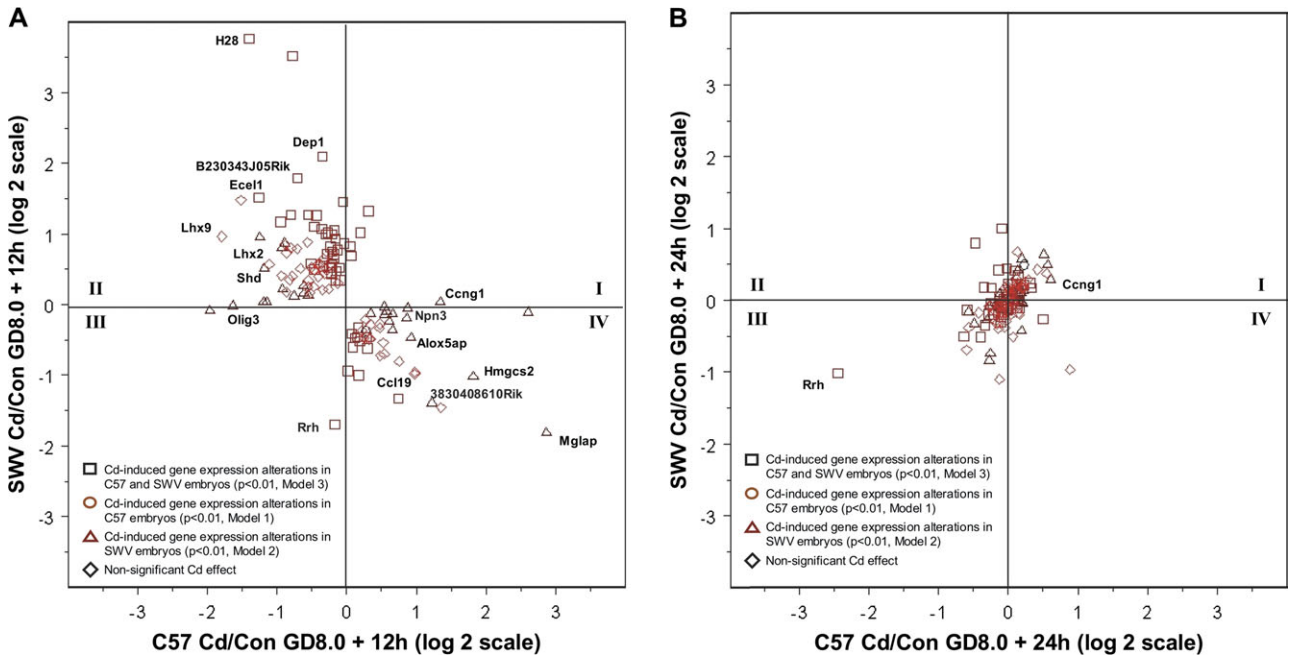

FIG. 3. Cd-induced gene expression alterations identified to be differentially impacted between C57 and SWV embryos. Scatter plots display the magnitude of change (Cd/Con) between Cd and control in 123 genes identified to be differentially impacted by Cd comparing C57 and SWV strains (12-h [A] and 24-h [B] p.i.). Genes were identified as statistically significant due to a significant BCd_Strain interaction term ($p < 0.01$) in Model 3. In addition, genes are labeled based on significant Cd effects identified in both strains (squares) (Model 3, B_{Cd}, $p < 0.01$), the C57 only (triangles) (Model 1, B_{Cd}, $p < 0.01$), the SWV only (circles) (Model 2, B_{Cd}, $p < 0.01$) or nonsignificant in any of the three models (diamonds).

Based upon observations of p53 and Cdkn1a Cd-induced gene expression changes, we evaluated gene expression changes in context of the p53 Signaling pathway to explore possible interactions between p53 and downstream mediators which regulate key processes such as angiogenesis, cell cycle arrest and apoptosis (Fig. 6). In this figure, we observed Cd-induced upregulation of p53 in both strains (shaded yellow) (Model 3, B_{Cd}, $p < 0.01$). In contrast, we observed upregulation of p53-downstream mediators Cdkn1a, Ccng1, and Pmaip1 in only the C57 (shaded red) (Model 1, B_{Cd}, $p < 0.01$). Additionally, this pathway revealed possible roles of p53 regulation via alterations in Akt2, Ctnnb1, Pik3cd, and Pten transcriptional changes. These genes were observed to be significantly altered in the C57 and the SWV (shaded yellow) (Model 3, B_{Cd}, $p < 0.01$). No genes were identified to be significantly altered in only the SWV linked with the canonical Ingenuity p53 Signaling pathway (shaded orange).

Validation of En2, Cdkn1a, and Pmaip1 Expression Using qRT-PCR

In Table 4, we validated microarray observations of Cd-induced changes in En2, Cdkn1a, Pmaip1, and Neurog2 expression using qRT-PCR. Similarly to our microarray results, we observed downregulation of the nervous system development-related gene, En2 in only the C57 at 12-h p.i. ($p < 0.05$). Likewise, we observed a significant increase in Pmaip1 and Cdkn1a in the C57 ($p < 0.05$). In contrast to our microarray results, which showed increased, but insignificant effects for Cd-induced Cdkn1a expression in the SWV, we observed a significant ~3× increase in Cdkn1a expression at 12-h p.i. ($p < 0.05$). Using microarray and qRT-PCR, we did not observe significant alterations in Neurog2 expression in either strain.

DISCUSSION

Similar to observations in C57BL/6NCrlBR and SWV/Fnn embryos exposed to Cd during neurulation (Hovland *et al.*, 1999), we observed differences in sensitivity between C57 (sensitive) and SWV (resistant) fetuses for endpoints of growth, resorptions, cranial neural tube closure, and the NTD exencephaly (Tables 1, 2). With this comparative mouse model, we investigated the impact of Cd on gene expression (GD 8.0 + 12 and 24 h) in parallel with cranial neural tube closure. We identified significantly altered genes and enriched biological processes via ANOVA and GO analysis to identify common and strain specific toxicogenomic responses that associated with developmental toxicity and sensitivity.

Correlated with Cd sensitivity, and thus also the incidence of NTD formation, we observed differential Cd-induced toxicogenomic responses between C57 and SWV embryos, corresponding with differential enriched GO terms and unique gene expression alterations. GO analysis suggested a more enriched response in nervous system development and cell cycle arrest-

TABLE 3
Cd-Induced Alterations in Gene Expression-Linked GO Biological Processes in C57 and SWV Embryos

					Model 1 (B_{Cd}, $p < 0.01$)			Model 2 (B_{Cd}, $p < 0.01$)		
Path	GO ID	GO name	#*M*	#GO	$\#C_{C57}$	Z_{C57}	P_{C57}	$\#C_{SWV}$	Z_{SWV}	P_{SWV}
0.0.1.0.1.3	51336	Regulation of hydrolase activity	72	105	6	3.5	0.005	4	0.2	1
0.0.1.0.1.3.4	43087	Regulation of GTPase activity	26	40	3	3.2	0.018	3	1.5	0.16
0.0.1.1.0.1.11	45786	Negative regulation of progression through cell cycle^	100	147	7	3.2	0.011	5	−0.1	1
0.0.1.1.0.1.11.0	7050	Cell cycle arrest^	38	68	4	3.4	0.013	1	−0.7	0.725
0.0.1.1.0.1.5	8285	Negative regulation of cell proliferation^	103	189	7	3.1	0.011	8	1.2	0.271
0.0.1.1.1.0.9.0.0.2.0	8630	DNA damage response\, signal trans induction of apop	12	15	0	−0.5	1	3	3.1	0.017
0.0.1.1.11	50794	Regulation of cellular process	2528	3752	69	1.8	0.092	155	2.5	0.017
0.0.1.1.11.3.0.0	75	Cell cycle checkpoint	19	47	0	−0.7	1	4	3.1	0.016
0.0.1.1.11.3.0.0.0	31570	DNA integrity checkpoint	11	26	0	−0.5	1	3	3.3	0.014
0.0.1.1.11.3.0.0.0.0	77	DNA damage checkpoint	10	22	0	−0.5	1	3	3.6	0.009
0.0.1.1.11.4.16	45667	Regulation of osteoblast differentiation	7	11	1	2.1	0.139	3	4.5	0.008
0.0.1.1.20	40029	Regulation of gene expression\, epigenetic	40	64	1	0.1	1	6	2.8	0.012
0.0.1.1.20.0	6306	DNA methylation	20	37	1	0.8	0.43	4	3.0	0.019
0.0.3.10	1708	Cell fate specification	19	25	1	0.9	0.332	4	3.1	0.013
0.0.3.17	16043	Cellular component organization and biogenesis	1640	2656	49	2.1	0.046	106	2.6	0.016
0.0.3.17.2.0.4.11	51169	Nuclear transport	75	115	2	0.2	1	9	2.7	0.019
0.0.3.17.2.0.4.11.1.0.2	60	Protein import into nucleus\, translocation	14	22	0	−0.6	1	4	4.0	0.003
0.0.3.17.2.0.4.7.0	65002	Intracellular protein transport across a membrane	14	22	0	−0.6	1	4	4.0	0.003
0.0.3.17.2.0.4.7.3	6605	Protein targeting	176	272	6	1.0	0.281	18	3.1	0.003
0.0.3.17.3	32989	Cellular structure morphogenesis	352	485	15	2.6	0.016	23	1.2	0.27
0.0.3.17.3.0	902	Cell morphogenesis	352	485	15	2.6	0.016	23	1.2	0.27
0.0.3.17.3.0.0	48858	Cell projection morphogenesis	191	249	10	2.8	0.014	11	0.4	0.752
0.0.3.17.3.0.0.0	30030	Cell projection organization and biogenesis	191	249	10	2.8	0.014	11	0.4	0.752
0.0.3.17.3.0.2	904	Cellular morphogenesis during differentiation	141	182	8	2.7	0.018	12	1.8	0.087
0.0.3.17.3.1	32990	Cell part morphogenesis	191	249	10	2.8	0.014	11	0.4	0.752
0.0.3.17.8	6996	Organelle organization and biogenesis	679	1201	17	0.4	0.667	52	3.0	0.005
0.0.3.17.8.1	51276	Chromosome organization and biogenesis	229	399	5	−0.1	1	21	2.8	0.012
0.0.3.17.8.1.1	7001	Chromosome organization and biogenesis (Eukaryota)	217	390	5	0.0	1	20	2.7	0.012
0.0.3.18	48869	Cellular developmental process	1528	2098	49	2.7	0.007	87	1.0	0.342
0.0.3.18.1	30154	Cell differentiation	1528	2098	49	2.7	0.007	87	1.0	0.342
0.0.3.3.3.0.1.2.7	48008	Platelet-derived growth factor receptor signaling pathway	4	5	0	−0.3	1	3	6.3	0
0.0.3.3.3.2.6	7243	Protein kinase cascade	223	328	1	−1.8	0.073	21	2.9	0.005
0.0.3.3.3.2.6.2	165	MAPKKK cascade	94	144	0	−1.5	0.197	11	2.9	0.01
0.0.3.3.3.2.6.2.4	7254	JNK cascade	34	51	0	−0.9	0.653	6	3.3	0.011
0.0.3.3.3.2.9	31098	Stress-activated protein kinase signaling pathway	35	54	0	−0.9	0.653	6	3.2	0.012
0.0.3.4	7049	Cell cycle$	492	762	15	1.2	0.279	41	3.2	0.002
0.0.3.4.0	22402	Cell cycle process$	394	646	13	1.4	0.168	32	2.7	0.008
0.0.3.4.0.0	22403	Cell cycle phase$	199	289	5	0.2	0.822	20	3.1	0.004
0.0.4	32502	Developmental process	2316	3292	71	2.9	0.009	131	1.2	0.274
0.0.4.2	48856	Anatomical structure development	1406	2002	46	2.7	0.009	80	0.9	0.402
0.0.5.2.2.2	17038	Protein import	64	93	0	−1.2	0.407	8	2.7	0.014
0.0.11	8152	Metabolic process	5409	8113	112	−1.3	0.21	314	2.9	0.004
0.0.11.3	44237	Cellular metabolic process	4847	7311	104	−0.7	0.535	284	2.9	0.007
0.0.11.3.11.2.10	6464	Protein modification process	1094	1609	23	−0.4	0.742	78	3.1	0.001
0.0.11.3.11.2.10.1	43687	Post-translational protein modification	950	1375	19	−0.6	0.653	70	3.2	0
0.0.11.3.11.2.10.1.14	6468	Protein amino acid phosphorylation	450	646	9	−0.4	0.754	40	3.6	0.001
0.0.11.3.19	6139	Nucleo-base,-side,-tide and nucleic acid meta process	2277	3483	54	0.4	0.689	150	3.4	0

TABLE 3—*Continued*

Path	GO ID	GO name	#*M*	#GO	Model 1 (B_{Cd}, $p < 0.01$) #C_{C57}	Z_{C57}	P_{C57}	Model 2 (B_{Cd}, $p < 0.01$) #C_{SWV}	Z_{SWV}	P_{SWV}
0.0.11.3.19.0	6259	DNA metabolic process	431	733	10	0.1	1	45	5.0	0
0.0.11.3.19.0.10	6260	DNA replication	103	161	3	0.4	0.74	12	3.0	0.01
0.0.11.3.19.0.10.1	6261	DNA-dependent DNA replication	40	73	1	0.1	1	9	5.0	0.003
0.0.11.3.19.0.10.1.0	6270	DNA replication initiation	13	26	0	−0.5	1	4	4.2	0.006
0.0.11.3.19.0.5.0	6305	DNA alkylation	20	37	1	0.8	0.43	4	3.0	0.019
0.0.11.3.19.0.6.0.0	6333	Chromatin assembly or disassembly	75	180	0	−1.3	0.257	9	2.7	0.013
0.0.11.3.19.0.9	6281	DNA repair	143	202	4	0.4	0.77	17	3.7	0.001
0.0.11.3.19.0.9.5	6302	Double-strand break repair	14	22	0	−0.6	1	4	4.0	0.005
0.0.11.3.24	6793	Phosphorus metabolic process	615	912	16	0.6	0.583	52	3.8	0
0.0.11.3.24.0	6796	Phosphate metabolic process	615	912	16	0.6	0.583	52	3.8	0
0.0.11.3.24.0.1	16310	Phosphorylation	509	760	13	0.5	0.632	42	3.2	0.001
0.0.11.3.30.0	6775	Fat-soluble vitamin metabolic process	21	27	3	3.7	0.011	1	−0.1	1
0.0.11.3.30.0.1	6776	Vitamin A metabolic process	16	21	3	4.4	0.005	1	0.2	1
0.0.11.5	43170	Macromolecule metabolic process	4175	6411	81	−1.7	0.1	254	3.3	0
0.0.11.5.0	43283	Biopolymer metabolic process	3081	4641	68	−0.2	0.857	206	4.4	0
0.0.11.5.0.2	43412	Biopolymer modification	1136	1677	23	−0.6	0.593	83	3.4	0
0.0.11.8	44238	Primary metabolic process	4833	7338	98	−1.4	0.171	287	3.2	0.002
0.0.12.13	7275	Multicellular organismal development	1575	2140	50	2.6	0.007	89	0.9	0.386
0.0.12.13.0.0.0.0.0	42733	Embryonic digit morphogenesis	9	12	0	−0.5	1	4	5.3	0.001
0.0.12.13.12.0	9798	Axis specification	10	17	0	−0.5	1	3	3.6	0.009
0.0.12.13.12.3.1	9953	Dorsal/ventral pattern formation	32	36	0	−0.9	0.658	6	3.5	0.003
0.0.12.13.16	48731	System development	1208	1704	39	2.4	0.011	69	0.9	0.387
0.0.12.13.16.1	7417	Central nervous system development*	151	224	11	4.2	0	12	1.6	0.13
0.0.12.13.16.1.1	7420	Brain development*	117	152	8	3.4	0.003	8	0.8	0.519
0.0.12.13.16.8	7399	Nervous system development*	438	658	21	3.6	0	30	1.6	0.13
0.0.12.13.16.8.6	22008	Neurogenesis*	249	330	14	3.6	0.003	15	0.6	0.554
0.0.12.13.16.8.6.0	48699	Generation of neurons*	233	307	13	3.4	0.004	14	0.6	0.647
0.0.12.13.16.8.6.0.3	30182	Neuron differentiation*	202	273	10	2.6	0.015	11	0.2	0.873
0.0.12.13.16.8.6.0.3.2	48666	Neuron development*	158	213	9	2.9	0.015	11	1.0	0.384
0.0.12.13.16.8.6.0.3.2.1	31175	Neurite development*	142	192	8	2.7	0.016	10	1.0	0.348
0.0.12.13.16.8.6.0.3.2.1.1	48812	Neurite morphogenesis*	127	166	8	3.1	0.009	10	1.4	0.237
0.0.12.13.16.8.6.0.3.2.1.1.0	7409	Axonogenesis*	119	158	8	3.3	0.008	10	1.6	0.158
0.0.12.13.16.8.6.0.3.2.3	48667	Neuron morphogenesis during differentiation*	127	166	8	3.1	0.009	10	1.4	0.237
0.0.12.13.16.8.6.0.4	1764	Neuron migration*	42	54	4	3.2	0.009	2	−0.1	1
0.0.12.13.16.9.14.3	42471	Ear morphogenesis	40	46	4	3.3	0.011	3	0.7	0.719
0.0.12.13.16.9.14.3.0	42472	Inner ear morphogenesis	36	42	4	3.6	0.008	3	0.9	0.433
0.0.18.10	9719	Response to endogenous stimulus	195	279	8	1.7	0.077	22	3.9	0.002
0.0.18.10.2	6974	Response to DNA damage stimulus	176	253	7	1.5	0.105	22	4.4	0.001
0.0.18.10.2.2	42770	DNA damage response\, signal transduction	26	40	0	−0.8	0.676	5	3.2	0.011
0.0.18.6.5.1.2	9411	Response to UV	22	20	3	3.6	0.007	3	1.8	0.098

Note. GO Analysis was performed using MAPPFinder for all 374 and 739 genes found to be significantly altered with Cd in C57 and SWV embryos within Models 1 and 2 (B_{Cd}, $p < 0.01$), respectively. Gene expression-linked GO categories are ordered by GO hierarchy (Path) and displayed with each specific GOID, # of genes significantly altered within each GOID (#*C*), # of genes within biological process measured on Codelink array (#*M*), # of genes within each GO category (biological process) (#GO), the *Z*-score associated with each GOID (*Z*), and permutation *p* value (*P*). Only GO IDs meeting criteria of a minimum of three genes changed and a *p* value < 0.02 were selected to be significantly enriched (shaded gray).

related genes within the C57 compared to the SWV (Table 3). Using cross-scatter plots and pathway mapping, we further explored relationships between strains within genes in these related categories.

Early nervous system development evolves due to the precise coordination of several gene networks which regulate processes such as neuronal proliferation, differentiation and migration. In this study, in only the C57, Cd significantly inhibited several genes which encode for factors critical for early nervous system development and neuronal differentiation (i.e., Zic 1) (Figs. 4A and 4B). Quantitative analysis (GOQuant) of downregulated nervous system development genes (Fig. 4C), suggested a greater reduction in these genes in the C57 compared to the SWV (12-h p.i.). These genes included, members of the Zic family (Zic1, Zic2) which mediate several aspects of early development, including neurogenesis and body patterning, En2, recognized to be essential for normal cerebellum development via Zic1/Wnt-

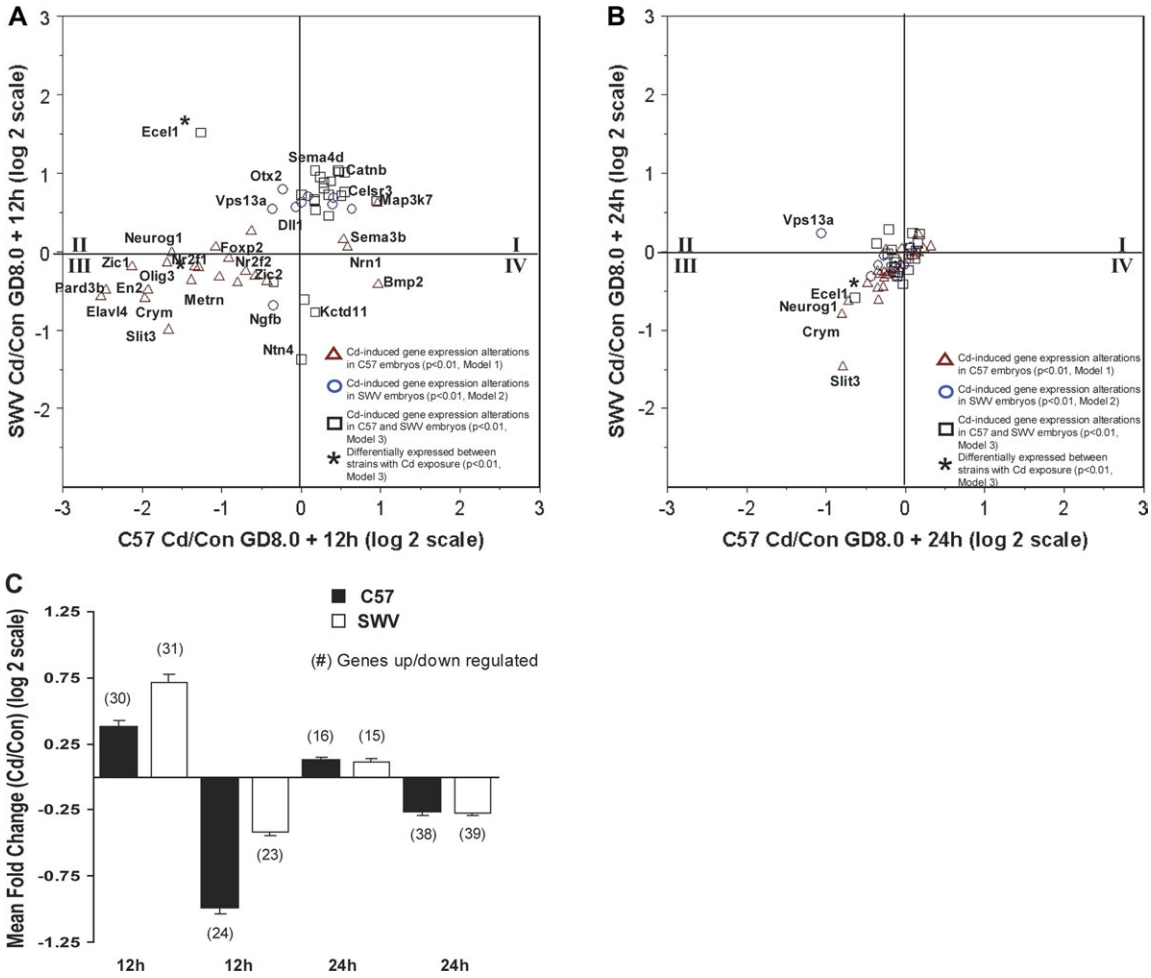

FIG. 4. Cd-induced gene expression alterations (Cd/con) in genes associated with Nervous System Development in C57 and SWV embryos. Cross-scatter plots of common and unique Cd-induced gene expression alterations in C57BL/6J and SWV embryos 12-h (A) and 24-h (B) p.i. (GD 8.0). The average Cd-induced fold change in all up- and downregulated nervous system development-related-genes (significant in either or both C57 and SWV embryos, Models 1–3; $p < 0.01$) (C). Genes labeled with an asterisk were identified to be significantly differentially altered by Cd between C57 and SWV embryos across time (Model 3, BCd_Strain, $p < 0.01$).

mediated signaling (Merzdorf and Sive, 2006; Nagai *et al.*, 1997), nuclear receptors (Nr2f2 and Nr2f1) important for proper axonal growth/migration and forebrain development (Armentano *et al.*, 2006; Tripodi *et al.*, 2004), Neurogenin 1 (Neurog1) involved in neuronal differentiation and neuronal survival through regulation of neuroD2 expression (Lin *et al.*, 2004) and the transcription factor, Olig3 which regulates oligodendrocyte differentiation and is expressed in the dorsal neural tube (Takebayashi *et al.*, 2002). Our gene expression results imply that Cd disrupts early neurogenesis/neurulation through disruption of transcription factors critical for nervous system development and furthermore, suggests that reduction in expression of specific genes critical for CNS development contributes to greater adverse developmental effects observed in the C57.

Metals such as Cd produce oxidative stress by interacting with cellular macromolecules resulting in lipid peroxidation, protein damage, DNA modifications and reactive oxygen species production (Bertin and Averbeck, 2006). Teratogen-induced forms of oxidative stress (including with Cd exposure) have been associated with NTDs (Li *et al.*, 2005; Paniagua-Castro *et al.*, 2007; Zhao and Reece, 2005), suggesting that the production of oxidative stress is highly detrimental to the neurulation process. In response to changes in redox status, several alterations in cellular homeostasis may result, including the disruption of cellular proliferation status (Hansen, 2006). As suggested by an extensive review (Copp, 2005), the exact mechanism by which alterations in cellular proliferation result in exencephaly is unclear, yet perturbed cell division may result in premature differentiation, disturbances in adhesion, changes in mechanical flexibility of the neural tube, suspended neural crest migration and other detrimental effects. Genetically deficient mouse models (Sah *et al.*, 1995) as well as environmental teratogens, such as Cd, arsenic and valproic acid (Dawson *et al.*, 2006; Fernandez *et al.*, 2003; Wlodarczyk *et al.*, 1996), suggest that alterations in cell cycle regulation

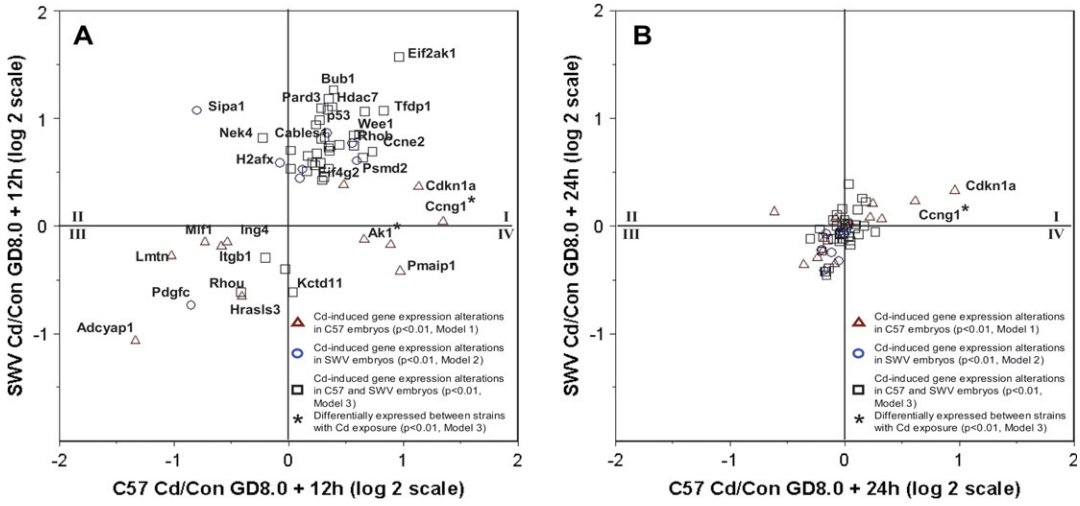

FIG. 5. Cd-induced gene expression alterations (Cd/con) in genes associated with cell cycle regulation in C57 and SWV embryos. Cross-scatter plots of common and unique Cd-induced gene expression cell cycle alterations in C57BL/6J and SWV embryos 12-h (A) and 24-h (B) p.i. (GD 8.0). Genes labeled with an asterisk were identified to be significantly differentially altered by Cd between C57 and SWV embryos (Model 3, BCd_Strain, $p < 0.01$).

correlate with disturbances in neurulation and the formation of exencephaly. In this study, in both strains, we observed Cd to induce significant changes in genes involved in cell cycle regulation (Table 3, Figs. 5, 6). Furthermore, within genes linked with cellular proliferation-related categories, we observed common and differential effects on expression correlating with differences in incidence of the NTD phenotype between the C57 and SWV (Figs. 5, 6).

The tumor suppressor gene p53 regulates the transcription of several genes involved in DNA repair, cell cycle arrest and apoptosis in response to environmentally mediated stress (Fig. 6). Several teratogens which induce NTDs activate p53 and p53-downstream mediators in embryos undergoing neurulation (Fernandez *et al*., 2003; Hosako *et al*., 2007; Wlodarczyk *et al*., 1996). In the cranial region of the neural tube, p53 (RNA and protein) and Cdkn1a (RNA) expression have been identified to be significantly increased at 24-h p.i. in C57 embryos (Fernandez *et al*., 2003). In this study, we observed a significant increase in p53 and Cdkn1a and other genes known to interact with p53, including Wee1, Parp1, Trp53bp1, Ccng1, and Pmaip1 (Fig. 5). However, these responses differed between the two strains. Genes known to be involved in p53-mediated DNA Repair (Parp1, Trp53bp1) and cell cycle arrest (Wee1) were observed to be upregulated (GD 8.0 + 12 h) in both strains (Fig. 5A), whereas Cdkn1a, Pmaip1, and Ccng1 were observed to be significantly altered in only the C57 strain (Figs. 5, 6). Follow-up validation using qRT-PCR revealed Cdkn1a to be significantly upregulated in both strains and confirmed differential expression of Pmaip1 (12-h p.i.) (Table 3).

Cdkn1a, Pmaip1, and Ccng1 may partake in differing roles in response to stress (Fig. 6). Cdkn1a induces cell cycle arrest by inhibiting cdk/cyclin complexes which promote G1/S and G2/M cell cycle transitions (Bartek and Lukas, 2001; Taylor and Stark, 2001), Pmaip1 advances cytochrome *c* release by interacting with bcl-like proteins on the mitochondrial membrane leading to caspase activation and apoptotic programming (Akhtar *et al*., 2006), whereas Ccng1 expression is associated with both cell cycle arrest and apoptosis (Okamoto and Prives, 1999; Zhao *et al*., 2003). A possible early indicator of stress in developing embryos, Cd induces Ccng1 RNA as early as 5 h in C57 embryos (p.i. on GD 8.0) (Kultima *et al*., 2006) and may be indicative of NTD formation as other teratogens, cyclophosphamide, and hyperthermia, induce elevation as well (Hosako *et al*., 2007). Our study suggests that genes involved in cell cycle regulation are affected in both strains, but that differential changes occur within this subset of genes, implicating that downstream mediators of p53 (i.e., Ccng1, Pmaip1) may correlate with differential response to Cd as observed between these two strains. Differential expression of these genes may be indicative of increased cell cycle arrest and apoptosis occurring in the C57 compared to the SWV.

In contrast to the GO-based approach to identify biological processes differentially impacted between strains as discussed above, additionally, we observed 123 genes to be significantly differentially impacted by Cd between strains using ANOVA to determine significant interactions between primary effects (Model 3, $B_{\text{Cd\_Strain}}$ $p < 0.01$). Four of these genes were linked with nervous system development or cell cycle GO terms (Ak1, Ccng1, Olig3, Ecel1), with several more implicated in development-related processes, including transcription regulators Lim/homeobox genes (Lhx9, Lhx2) and RAR-related orphan receptor alpha (Rora) (Bertuzzi *et al*., 1999; Dussault *et al*., 1998) (Supplemental Table 1). Differential impact on these genes may also manifest differential toxicogenomic responses observed between C57 and SWV strains.

In general, across both strains, we observed greater effects on gene expression due to Cd at 12-h p.i. compared to 24-h p.i. (Figs. 2, 3). Our observations associate with studies indicating

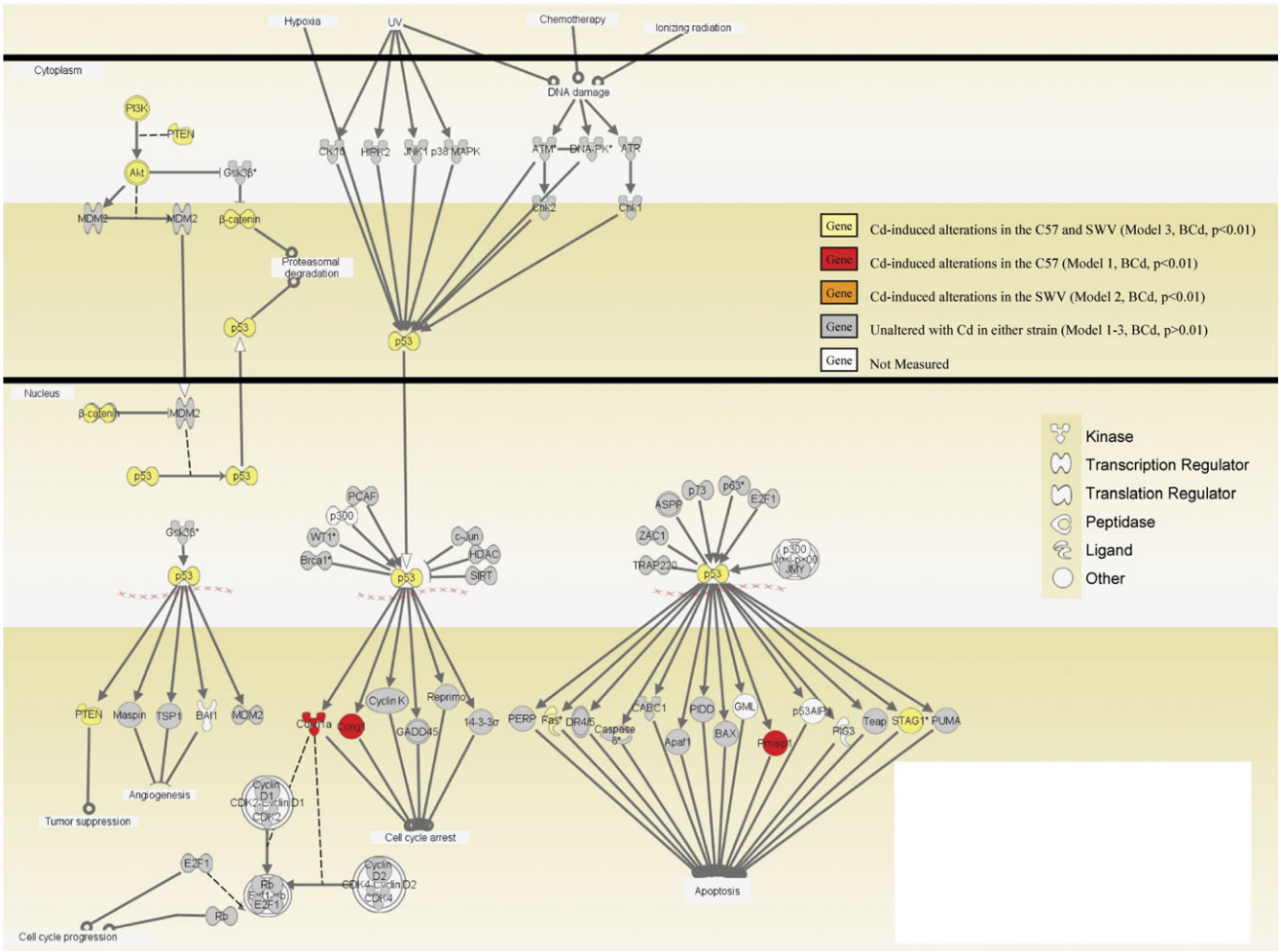

FIG. 6. Cd-induced alterations within the ingenuity canonical p53-signaling pathway in C57BL/6J and SWV embryos. Cd-induced alterations in C57 and SWV embryos were mapped to the p53 Signaling canonical ingenuity pathway (w/modifications). Genes are color coded based on Cd-effect specificity. Shapes of genes indicate known functions.

greater morphological changes (increased pyknotic nuclei) in cells along the neural tube at 10- to 12-h p.i. (GD 8.0, Cd) compared to later assessments (24-h, 48-h p.i.) (Webster and Messerle, 1980). Interestingly, most molecular studies have identified Cd-induced molecular perturbations at 24-h p.i., including markers of CNS development (Sox2), cell cycle regulation (p53, Cdkn1a) and apoptosis (bax, bcl2, c-casp3) (Fernandez *et al*., 2003, 2004). Earlier assessments may be of interest to identify sensitive markers of toxicity and upstream mechanisms which initially drive these potential responses. Yet, under similar exposure conditions as our study (Cd, 4 mg/kg BW, GD 8.0, C57) a recent microarray study only identified nine genes to be significantly altered at 5-h p.i. with Cd ($p < 0.05$, Abs fold change > 1.4) (Kultima *et al*., 2006), implying a small window to detect robust changes using current methodology and providing insight in combination with our study into the temporal response associated with Cd toxicity.

In this study, the observed differential embryonic gene expression response to Cd between C57 and SWV may be driven by multiple embryonic and maternal factors. Initial studies should address potential Cd toxicokinetic and metabolic differences between strains and regulators of ion homeostasis (Zn^{2+}), such as metallothioneins and/or ion transporters, which may influence placental or embryonic Cd accumulation.

Furthermore, although the process of neurulation is highly conserved between strains, subtle developmental differences may exist which underlie strain sensitivity. We observed no significant differences in closure of the neural tube (mid/hind brain region) between GD 8.5 and 9.0 in these two strains (Table 2). Likewise, earlier studies suggest similar developmental progress (somite counts) between these two strains during neurulation (Kuczuk and Scott, 1984). Future studies should examine for potential developmental temporal differences in gene expression across neurulation between inbred strains to search for clues which may correlate with sensitivity to teratogens.

Follow-up molecular studies assessing RNA and/or protein will be needed to establish localization and potential

TABLE 4
Secondary Validation of Gene Expression Alterations Using qRT-PCR

	qRT-PCR (log_2 ratio, Cd/Con)		Microarray (log_2 ratio, Cd/Con)	
Gene	C57	SWV	C57	SWV
En2	−1.30 ± 0.36*	−0.06 ± 0.38	−1.92 ± 0.40†	−0.48 ± 0.27
Cdkn1a	1.13 ± 0.23*	1.60 ± 0.25*	1.14 ± 0.35†	0.37 ± 0.14
Pmaip1	2.17 ± 0.07*	−0.40 ± 0.18	0.89 ± 0.19†	−0.17 ± 0.22
Neurog2	−0.55 ± 0.32	0.26 ± 0.35	−1.46 ± 0.56	0.33 ± 0.42

Note. To validate Cd-induced gene expression alterations identified using the Codelink platform, we conducted qRT-PCR for En2, Cdkn1a, Pmaip1, and Neurog2. All initial intensity values were adjusted by Gadph intensity, used as an internal housekeeping gene. Log 2 ratios represent comparisons between Cd-exposed and control C57 and SWV embryos 12-h p.i. ($n = 3$–4). Asterisks signify significant effects assessed using two-sided *t*-test ($p < 0.05$). Crosses indicate genes identified as significantly altered ($p < 0.01$) by Cd across the two time points assessed in our microarray study (12-, 24-h p.i.). Neurog2 was assessed to compare fold change values in a gene which was not identified to be significantly altered in our microarray study.

interactions of the proposed targets in this study. Integrating results from this dataset with pre-established gene expression databases such as the EMAGE library (Christiansen *et al*., 2006) may provide clues of localization of targets during early neurulation and CNS development. For example, expression of nervous system development targets (En2, Zic 1) identified to be downregulated following Cd exposure in the C57 are normally expressed in several regions of the embryo, including the neuroectodermal layer of the cranial neural tube (not shown), supporting the hypothesis that expression of these genes are affected by Cd in regions of the cranial neural tube.

In this study, we present a toxicogenomic approach to methodically identify teratogenic responses which associate with differential sensitivity using resistant and sensitive mouse embryos. In conclusion, this study extends previous observations associating alterations in development, cell cycle and apoptotic processes with environmental teratogens and developmental toxicity (NTDs, mortality, growth) and furthermore, provides insight into the key mechanisms and specific genes that underlie differences in response to teratogens. Results from this study will support future studies investigating time-dependent and dose-response analyses, proteomic alterations, and localization of expression of identified targets and their potential link with NTD formation as well as gene-environment interactions associated with sensitivity.

SUPPLEMENTARY DATA

Supplementary data are available online at http://toxsci.oxfordjournals.org/

FUNDING

National Institute of Environmental Health Sciences (NIEHS) (Toxicogenomics, U10 ES 11387 and R01-ES10613); the U.S. Environmental Protection Agency-NIEHS UW Center for Child Environmental Health Risks Research (EPA R826886 and NIEHS 1PO1ES09601); the Center for Oceans and Human Health Research (NIEHS: P50 ES012762 and National Science Foundation (NSF: OCE-0434087); and the UW NIEHS Center for Ecogenetics and Environmental Health (5 P30 ES07033).

ACKNOWLEDGMENTS

We wish to thank Rob Sullivan, Helmut Zarbl, and Theo Bammler for assisting in various aspects of the microarray process; Fred Farin and Jasmine Wilkerson for help with conducting the qRT-PCR experiments; and Phillip Mirkes and Richard Finnell for supplying the original SWV mice to establish our colony at the University of Washington.

REFERENCES

Akhtar, R. S., Geng, Y., Klocke, B. J., Latham, C. B., Villunger, A., Michalak, E. M., Strasser, A., Carroll, S. L., and Roth, K. A. (2006). BH3-only proapoptotic Bcl-2 family members Noxa and Puma mediate neural precursor cell death. *J. Neurosci*. **26,** 7257–7264.

Armentano, M., Filosa, A., Andolfi, G., and Studer, M. (2006). COUP-TFI is required for the formation of commissural projections in the forebrain by regulating axonal growth. *Development* **133,** 4151–4162.

Bartek, J., and Lukas, J. (2001). Pathways governing G1/S transition and their response to DNA damage. *FEBS Lett*. **490,** 117–122.

Bertin, G., and Averbeck, D. (2006). Cadmium: Cellular effects, modifications of biomolecules, modulation of DNA repair and genotoxic consequences (a review). *Biochimie* **88,** 1549–1559.

Bertuzzi, S., Porter, F. D., Pitts, A., Kumar, M., Agulnick, A., Wassif, C., and Westphal, H. (1999). Characterization of Lhx9, a novel LIM/homeobox gene expressed by the pioneer neurons in the mouse cerebral cortex. *Mech. Dev*. **81,** 193–198.

Brender, J. D., Suarez, L., Felkner, M., Gilani, Z., Stinchcomb, D., Moody, K., Henry, J., and Hendricks, K. (2006). Maternal exposure to arsenic, cadmium, lead, and mercury and neural tube defects in offspring. *Environ. Res*. **101,** 132–139.

Christiansen, J. H., Yang, Y., Venkataraman, S., Richardson, L., Stevenson, P., Burton, N., Baldock, R. A., and Davidson, D. R. (2006). EMAGE: A spatial database of gene expression patterns during mouse embryo development. *Nucleic Acids Res*. **34,** D637–D641.

Christley, J., and Webster, W. S. (1983). Cadmium uptake and distribution in mouse embryos following maternal exposure during the organogenic period: A scintillation and autoradiographic study. *Teratology* **27,** 305–312.

Copp, A. J. (2005). Neurulation in the cranial region–normal and abnormal. *J. Anat*. **207,** 623–635.

Danielsson, B. R., and Dencker, L. (1984). Effects of cadmium on the placental uptake and transport to the fetus of nutrients. *Biol. Res. Pregnancy Perinatol*. **5,** 93–101.

Dawson, J. E., Raymond, A. M., and Winn, L. M. (2006). Folic acid and pantothenic acid protection against valproic acid-induced neural tube defects in CD-1 mice. *Toxicol. Appl. Pharmacol.* **211,** 124–132.

Dencker, L. (1975). Possible mechanisms of cadmium fetotoxicity in golden hamsters and mice: Uptake by the embryo, placenta and ovary. *J. Reprod. Fertil.* **44,** 461–471.

Doniger, S. W., Salomonis, N., Dahlquist, K. D., Vranizan, K., Lawlor, S. C., and Conklin, B. R. (2003). MAPPFinder: Using Gene Ontology and GenMAPP to create a global gene-expression profile from microarray data. *Genome Biol.* **4,** R7.

Dussault, I., Fawcett, D., Matthyssen, A., Bader, J. A., and Giguere, V. (1998). Orphan nuclear receptor ROR alpha-deficient mice display the cerebellar defects of staggerer. *Mech. Dev.* **70,** 147–153.

Ferm, V. H. (1971). Developmental malformations induced by cadmium. A study of timed injections during embryogenesis. *Biol. Neonate* **19,** 101–107.

Ferm, V. H., and Carpenter, S. J. (1968). The relationship of cadmium and zinc in experimental mammalian teratogenesis. *Lab. Invest.* **18,** 429–432.

Fernandez, E. L., Gustafson, A. L., Andersson, M., Hellman, B., and Dencker, L. (2003). Cadmium-induced changes in apoptotic gene expression levels and DNA damage in mouse embryos are blocked by zinc. *Toxicol. Sci.* **76,** 162–170.

Fernandez, E. L., Svenson, C., Dencker, L., and Gustafson, A. L. (2004). Disturbing endoderm signaling to anterior neural plate of vertebrates by the teratogen cadmium. *Reprod. Toxicol.* **18,** 653–660.

Finnell, R. H., Moon, S. P., Abbott, L. C., Golden, J. A., and Chernoff, G. F. (1986). Strain differences in heat-induced neural tube defects in mice. *Teratology* **33,** 247–252.

Finnell, R. H., Shields, H. E., Taylor, S. M., and Chernoff, G. F. (1987). Strain differences in phenobarbital-induced teratogenesis in mice. *Teratology* **35,** 177–185.

Frey, L., and Hauser, W. A. (2003). Epidemiology of neural tube defects. *Epilepsia* **44**(Suppl. 3), 4–13.

Hansen, J. M. (2006). Oxidative stress as a mechanism of teratogenesis. *Birth Defects Res. C Embryo Today* **78,** 293–307.

Harris, M. J., and Juriloff, D. M. (2007). Mouse mutants with neural tube closure defects and their role in understanding human neural tube defects. *Birth Defects Res. A Clin. Mol. Teratol.* **79,** 187–210.

Hosako, H., Little, S. A., Barrier, M., and Mirkes, P. E. (2007). Teratogen-induced activation of p53 in early postimplantation mouse embryos. *Toxicol. Sci.* **95,** 257–269.

Hovland, D. N., Jr., Cantor, R. M., Lee, G. S., Machado, A. F., and Collins, M. D. (2000). Identification of a murine locus conveying susceptibility to cadmium-induced forelimb malformations. *Genomics* **63,** 193–201.

Hovland, D. N., Jr., Machado, A. F., Scott, W. J., Jr., and Collins, M. D. (1999). Differential sensitivity of the SWV and C57BL/6 mouse strains to the teratogenic action of single administrations of cadmium given throughout the period of anterior neuropore closure. *Teratology* **60,** 13–21.

Kuczuk, M. H., and Scott, W. J., Jr. (1984). Potentiation of acetazolamide induced ectrodactyly in SWV and C57BL/6J mice by cadmium sulfate. *Teratology* **29,** 427–435.

Kultima, K., Fernandez, E. L., Scholz, B., Gustafson, A. L., Dencker, L., and Stigson, M. (2006). Cadmium-induced gene expression changes in the mouse embryo, and the influence of pretreatment with zinc. *Reprod. Toxicol.* **22,** 636–646.

Li, R., Chase, M., Jung, S. K., Smith, P. J., and Loeken, M. R. (2005). Hypoxic stress in diabetic pregnancy contributes to impaired embryo gene expression and defective development by inducing oxidative stress. *Am. J. Physiol. Endocrinol. Metab.* **289,** E591–E599.

Lin, C. H., Stoeck, J., Ravanpay, A. C., Guillemot, F., Tapscott, S. J., and Olson, J. M. (2004). Regulation of neuroD2 expression in mouse brain. *Dev. Biol.* **265,** 234–245.

Lundberg, Y. W., Cabrera, R. M., Greer, K. A., Zhao, J., Garg, R., and Finnell, R. H. (2004). Mapping a chromosomal locus for valproic acid-induced exencephaly in mice. *Mamm. Genome* **15,** 361–369.

Lundberg, Y. W., Wing, M. J., Xiong, W., Zhao, J., and Finnell, R. H. (2003). Genetic dissection of hyperthermia-induced neural tube defects in mice. *Birth Defects Res. A Clin. Mol. Teratol.* **67,** 409–413.

Machado, A. F., Hovland, D. N., Jr., Pilafas, S., and Collins, M. D. (1999). Teratogenic response to arsenite during neurulation: Relative sensitivities of C57BL/6J and SWV/Fnn mice and impact of the splotch allele. *Toxicol. Sci.* **51,** 98–107.

Merzdorf, C. S., and Sive, H. L. (2006). The zic1 gene is an activator of Wnt signaling. *Int. J. Dev. Biol.* **50,** 611–617.

Nagai, T., Aruga, J., Takada, S., Gunther, T., Sporle, R., Schughart, K., and Mikoshiba, K. (1997). The expression of the mouse Zic1, Zic2, and Zic3 gene suggests an essential role for Zic genes in body pattern formation. *Dev. Biol.* **182,** 299–313.

Naruse, I., Collins, M. D., and Scott, W. J., Jr. (1988). Strain differences in the teratogenicity induced by sodium valproate in cultured mouse embryos. *Teratology* **38,** 87–96.

Nassau, J. H., and Drotar, D. (1997). Social competence among children with central nervous system-related chronic health conditions: A review. *J. Pediatr. Psychol.* **22,** 771–793.

Okamoto, K., and Prives, C. (1999). A role of cyclin G in the process of apoptosis. *Oncogene* **18,** 4606–4615.

Paniagua-Castro, N., Escalona-Cardoso, G., and Chamorro-Cevallos, G. (2007). Glycine reduces cadmium-induced teratogenic damage in mice. *Reprod. Toxicol.* **23,** 92–97.

Ronco, A. M., Arguello, G., Munoz, L., Gras, N., and Llanos, M. (2005). Metals content in placentas from moderate cigarette consumers: Correlation with newborn birth weight. *Biometals* **18,** 233–241.

Sah, V. P., Attardi, L. D., Mulligan, G. J., Williams, B. O., Bronson, R. T., and Jacks, T. (1995). A subset of p53-deficient embryos exhibit exencephaly. *Nat. Genet.* **10,** 175–180.

Takebayashi, H., Ohtsuki, T., Uchida, T., Kawamoto, S., Okubo, K., Ikenaka, K., Takeichi, M., Chisaka, O., and Nabeshima, Y. (2002). Non-overlapping expression of Olig3 and Olig2 in the embryonic neural tube. *Mech. Dev.* **113,** 169–174.

Taylor, W. R., and Stark, G. R. (2001). Regulation of the G2/M transition by p53. *Oncogene* **20,** 1803–1815.

Tripodi, M., Filosa, A., Armentano, M., and Studer, M. (2004). The COUP-TF nuclear receptors regulate cell migration in the mammalian basal forebrain. *Development* **131,** 6119–6129.

Webster, W. S., and Messerle, K. (1980). Changes in the mouse neuro-epithelium associated with cadmium-induced neural tube defects. *Teratology* **21,** 79–88.

Wlodarczyk, B. C., Craig, J. C., Bennett, G. D., Calvin, J. A., and Finnell, R. H. (1996). Valproic acid-induced changes in gene expression during neurulation in a mouse model. *Teratology* **54,** 284–297.

Yu, X., Griffith, W. C., Hanspers, K., Dillman, J. F., 3rd., Ong, H., Vredevoogd, M. A., and Faustman, E. M. (2006). A system-based approach to interpret dose- and time-dependent microarray data: Quantitative integration of gene ontology analysis for risk assessment. *Toxicol. Sci.* **92,** 560–577.

Zhao, L., Samuels, T., Winckler, S., Korgaonkar, C., Tompkins, V., Horne, M. C., and Quelle, D. E. (2003). Cyclin G1 has growth inhibitory activity linked to the ARF-Mdm2-p53 and pRb tumor suppressor pathways. *Mol. Cancer Res.* **1,** 195–206.

Zhao, Z., and Reece, E. A. (2005). Nicotine-induced embryonic malformations mediated by apoptosis from increasing intracellular calcium and oxidative stress. *Birth Defects Res. A Clin. Mol. Teratol.* **74,** 383–391.